Search for Lepton-Flavor and Lepton-Number Violation in the Decay $\tau^- \to \ell^\mp h^\pm h'^-$

B. Aubert,[1] R. Barate,[1] D. Boutigny,[1] F. Couderc,[1] Y. Karyotakis,[1] J. P. Lees,[1] V. Poireau,[1] V. Tisserand,[1] A. Zghiche,[1] E. Grauges,[2] A. Palano,[3] M. Pappagallo,[3] A. Pompili,[3] J. C. Chen,[4] N. D. Qi,[4] G. Rong,[4] P. Wang,[4] Y. S. Zhu,[4] G. Eigen,[5] I. Ofte,[5] B. Stugu,[5] G. S. Abrams,[6] M. Battaglia,[6] A. B. Breon,[6] D. N. Brown,[6] J. Button-Shafer,[6] R. N. Cahn,[6] E. Charles,[6] C. T. Day,[6] M. S. Gill,[6] A. V. Gritsan,[6] Y. Groysman,[6] R. G. Jacobsen,[6] R. W. Kadel,[6] J. Kadyk,[6] L. T. Kerth,[6] Yu. G. Kolomensky,[6] G. Kukartsev,[6] G. Lynch,[6] L. M. Mir,[6] P. J. Oddone,[6] T. J. Orimoto,[6] M. Pripstein,[6] N. A. Roe,[6] M. T. Ronan,[6] W. A. Wenzel,[6] M. Barrett,[7] K. E. Ford,[7] T. J. Harrison,[7] A. J. Hart,[7] C. M. Hawkes,[7] S. E. Morgan,[7] A. T. Watson,[7] M. Fritsch,[8] K. Goetzen,[8] T. Held,[8] H. Koch,[8] B. Lewandowski,[8] M. Pelizaeus,[8] K. Peters,[8] T. Schroeder,[8] M. Steinke,[8] J. T. Boyd,[9] J. P. Burke,[9] N. Chevalier,[9] W. N. Cottingham,[9] M. P. Kelly,[9] T. Cuhadar-Donszelmann,[10] B. G. Fulsom,[10] C. Hearty,[10] N. S. Knecht,[10] T. S. Mattison,[10] J. A. McKenna,[10] A. Khan,[11] P. Kyberd,[11] M. Saleem,[11] L. Teodorescu,[11] A. E. Blinov,[12] V. E. Blinov,[12] A. D. Bukin,[12] V. P. Druzhinin,[12] V. B. Golubev,[12] E. A. Kravchenko,[12] A. P. Onuchin,[12] S. I. Serednyakov,[12] Yu. I. Skovpen,[12] E. P. Solodov,[12] A. N. Yushkov,[12] D. Best,[13] M. Bondioli,[13] M. Bruinsma,[13] M. Chao,[13] I. Eschrich,[13] D. Kirkby,[13] A. J. Lankford,[13] M. Mandelkern,[13] R. K. Mommsen,[13] W. Roethel,[13] D. P. Stoker,[13] C. Buchanan,[14] B. L. Hartfiel,[14] A. J. R. Weinstein,[14] S. D. Foulkes,[15] J. W. Gary,[15] O. Long,[15] B. C. Shen,[15] K. Wang,[15] L. Zhang,[15] D. del Re,[16] H. K. Hadavand,[16] E. J. Hill,[16] D. B. MacFarlane,[16] H. P. Paar,[16] S. Rahatlou,[16] V. Sharma,[16] J. W. Berryhill,[17] C. Campagnari,[17] A. Cunha,[17] B. Dahmes,[17] T. M. Hong,[17] M. A. Mazur,[17] J. D. Richman,[17] W. Verkerke,[17] T. W. Beck,[18] A. M. Eisner,[18] C. J. Flacco,[18] C. A. Heusch,[18] J. Kroseberg,[18] W. S. Lockman,[18] G. Nesom,[18] T. Schalk,[18] B. A. Schumm,[18] A. Seiden,[18] P. Spradlin,[18] D. C. Williams,[18] M. G. Wilson,[18] J. Albert,[19] E. Chen,[19] G. P. Dubois-Felsmann,[19] A. Dvoretskii,[19] D. G. Hitlin,[19] I. Narsky,[19] T. Piatenko,[19] F. C. Porter,[19] A. Ryd,[19] A. Samuel,[19] R. Andreassen,[20] S. Jayatilleke,[20] G. Mancinelli,[20] B. T. Meadows,[20] M. D. Sokoloff,[20] F. Blanc,[21] P. Bloom,[21] S. Chen,[21] W. T. Ford,[21] U. Nauenberg,[21] A. Olivas,[21] P. Rankin,[21] W. O. Ruddick,[21] J. G. Smith,[21] K. A. Ulmer,[21] S. R. Wagner,[21] J. Zhang,[21] A. Chen,[22] E. A. Eckhart,[22] A. Soffer,[22] W. H. Toki,[22] R. J. Wilson,[22] Q. Zeng,[22] D. Altenburg,[23] E. Feltresi,[23] A. Hauke,[23] B. Spaan,[23] T. Brandt,[24] J. Brose,[24] M. Dickopp,[24] V. Klose,[24] H. M. Lacker,[24] R. Nogowski,[24] S. Otto,[24] A. Petzold,[24] G. Schott,[24] J. Schubert,[24] K. R. Schubert,[24] R. Schwierz,[24] J. E. Sundermann,[24] D. Bernard,[25] G. R. Bonneaud,[25] P. Grenier,[25] S. Schrenk,[25] Ch. Thiebaux,[25] G. Vasileiadis,[25] M. Verderi,[25] D. J. Bard,[26] P. J. Clark,[26] W. Gradl,[26] F. Muheim,[26] S. Playfer,[26] Y. Xie,[26] M. Andreotti,[27] V. Azzolini,[27] D. Bettoni,[27] C. Bozzi,[27] R. Calabrese,[27] G. Cibinetto,[27] E. Luppi,[27] M. Negrini,[27] L. Piemontese,[27] F. Anulli,[28] R. Baldini-Ferroli,[28] A. Calcaterra,[28] R. de Sangro,[28] G. Finocchiaro,[28] P. Patteri,[28] I. M. Peruzzi,[28,*] M. Piccolo,[28] A. Zallo,[28] A. Buzzo,[29] R. Capra,[29] R. Contri,[29] M. Lo Vetere,[29] M. Macri,[29] M. R. Monge,[29] S. Passaggio,[29] C. Patrignani,[29] E. Robutti,[29] A. Santroni,[29] S. Tosi,[29] S. Bailey,[30] G. Brandenburg,[30] K. S. Chaisanguanthum,[30] M. Morii,[30] E. Won,[30] J. Wu,[30] R. S. Dubitzky,[31] U. Langenegger,[31] J. Marks,[31] S. Schenk,[31] U. Uwer,[31] W. Bhimji,[32] D. A. Bowerman,[32] P. D. Dauncey,[32] U. Egede,[32] R. L. Flack,[32] J. R. Gaillard,[32] G. W. Morton,[32] J. A. Nash,[32] M. B. Nikolich,[32] G. P. Taylor,[32] W. P. Vazquez,[32] M. J. Charles,[33] W. F. Mader,[33] U. Mallik,[33] A. K. Mohapatra,[33] J. Cochran,[34] H. B. Crawley,[34] V. Eyges,[34] W. T. Meyer,[34] S. Prell,[34] E. I. Rosenberg,[34] A. E. Rubin,[34] J. Yi,[34] N. Arnaud,[35] M. Davier,[35] X. Giroux,[35] G. Grosdidier,[35] A. Höcker,[35] F. Le Diberder,[35] V. Lepeltier,[35] A. M. Lutz,[35] A. Oyanguren,[35] T. C. Petersen,[35] M. Pierini,[35] S. Plaszczynski,[35] S. Rodier,[35] P. Roudeau,[35] M. H. Schune,[35] A. Stocchi,[35] G. Wormser,[35] C. H. Cheng,[36] D. J. Lange,[36] M. C. Simani,[36] D. M. Wright,[36] A. J. Bevan,[37] C. A. Chavez,[37] J. P. Coleman,[37] I. J. Forster,[37] J. R. Fry,[37] E. Gabathuler,[37] R. Gamet,[37] K. A. George,[37] D. E. Hutchcroft,[37] R. J. Parry,[37] D. J. Payne,[37] K. C. Schofield,[37] C. Touramanis,[37] C. M. Cormack,[38] F. Di Lodovico,[38] R. Sacco,[38] C. L. Brown,[39] G. Cowan,[39] H. U. Flaecher,[39] M. G. Green,[39] D. A. Hopkins,[39] P. S. Jackson,[39] T. R. McMahon,[39] S. Ricciardi,[39] F. Salvatore,[39] D. Brown,[40] C. L. Davis,[40] J. Allison,[41] N. R. Barlow,[41] R. J. Barlow,[41] M. C. Hodgkinson,[41] G. D. Lafferty,[41] M. T. Naisbit,[41] J. C. Williams,[41] C. Chen,[42] A. Farbin,[42] W. D. Hulsbergen,[42] A. Jawahery,[42] D. Kovalskyi,[42] C. K. Lae,[42] V. Lillard,[42] D. A. Roberts,[42] G. Simi,[42] G. Blaylock,[43] C. Dallapiccola,[43] S. S. Hertzbach,[43] R. Kofler,[43] V. B. Koptchev,[43] X. Li,[43] T. B. Moore,[43] S. Saremi,[43] H. Staengle,[43] S. Willocq,[43] R. Cowan,[44] K. Koeneke,[44] G. Sciolla,[44] S. J. Sekula,[44] M. Spitznagel,[44] F. Taylor,[44] R. K. Yamamoto,[44] H. Kim,[45] P. M. Patel,[45] S. H. Robertson,[45] A. Lazzaro,[46] V. Lombardo,[46] F. Palombo,[46] J. M. Bauer,[47] L. Cremaldi,[47] V. Eschenburg,[47] R. Godang,[47] R. Kroeger,[47] J. Reidy,[47] D. A. Sanders,[47] D. J. Summers,[47] H. W. Zhao,[47] S. Brunet,[48] D. Côté,[48] P. Taras,[48] B. Viaud,[48] H. Nicholson,[49] N. Cavallo,[50,†] G. De Nardo,[50] F. Fabozzi,[50,†] C. Gatto,[50] L. Lista,[50] D. Monorchio,[50] P. Paolucci,[50] D. Piccolo,[50] C. Sciacca,[50] M. Baak,[51] H. Bulten,[51] G. Raven,[51] H. L. Snoek,[51] L. Wilden,[51] C. P. Jessop,[52] J. M. LoSecco,[52] T. Allmendinger,[53] G. Benelli,[53] K. K. Gan,[53] K. Honscheid,[53] D. Hufnagel,[53]

P. D. Jackson,[53] H. Kagan,[53] R. Kass,[53] T. Pulliam,[53] A. M. Rahimi,[53] R. Ter-Antonyan,[53] Q. K. Wong,[53] J. Brau,[54] R. Frey,[54] O. Igonkina,[54] M. Lu,[54] C. T. Potter,[54] N. B. Sinev,[54] D. Strom,[54] J. Strube,[54] E. Torrence,[54] A. Dorigo,[55] F. Galeazzi,[55] M. Margoni,[55] M. Morandin,[55] M. Posocco,[55] M. Rotondo,[55] F. Simonetto,[55] R. Stroili,[55] C. Voci,[55] M. Benayoun,[56] H. Briand,[56] J. Chauveau,[56] P. David,[56] L. Del Buono,[56] Ch. de la Vaissière,[56] O. Hamon,[56] M. J. J. John,[56] Ph. Leruste,[56] J. Malclès,[56] J. Ocariz,[56] L. Roos,[56] G. Therin,[56] P. K. Behera,[57] L. Gladney,[57] Q. H. Guo,[57] J. Panetta,[57] M. Biasini,[58] R. Covarelli,[58] S. Pacetti,[58] M. Pioppi,[58] C. Angelini,[59] G. Batignani,[59] S. Bettarini,[59] F. Bucci,[59] G. Calderini,[59] M. Carpinelli,[59] R. Cenci,[59] F. Forti,[59] M. A. Giorgi,[59] A. Lusiani,[59] G. Marchiori,[59] M. Morganti,[59] N. Neri,[59] E. Paoloni,[59] M. Rama,[59] G. Rizzo,[59] J. Walsh,[59] M. Haire,[60] D. Judd,[60] D. E. Wagoner,[60] J. Biesiada,[61] N. Danielson,[61] P. Elmer,[61] Y. P. Lau,[61] C. Lu,[61] J. Olsen,[61] A. J. S. Smith,[61] A. V. Telnov,[61] F. Bellini,[62] G. Cavoto,[62] A. D'Orazio,[62] E. Di Marco,[62] R. Faccini,[62] F. Ferrarotto,[62] F. Ferroni,[62] M. Gaspero,[62] L. Li Gioi,[62] M. A. Mazzoni,[62] S. Morganti,[62] G. Piredda,[62] F. Polci,[62] F. Safai Tehrani,[62] C. Voena,[62] H. Schröder,[63] G. Wagner,[63] R. Waldi,[63] T. Adye,[64] N. De Groot,[64] B. Franek,[64] G. P. Gopal,[64] E. O. Olaiya,[64] F. F. Wilson,[64] R. Aleksan,[65] S. Emery,[65] A. Gaidot,[65] S. F. Ganzhur,[65] P.-F. Giraud,[65] G. Graziani,[65] G. Hamel de Monchenault,[65] W. Kozanecki,[65] M. Legendre,[65] G. W. London,[65] B. Mayer,[65] G. Vasseur,[65] Ch. Yèche,[65] M. Zito,[65] M. V. Purohit,[66] A. W. Weidemann,[66] J. R. Wilson,[66] F. X. Yumiceva,[66] T. Abe,[67] M. T. Allen,[67] D. Aston,[67] R. Bartoldus,[67] N. Berger,[67] A. M. Boyarski,[67] O. L. Buchmueller,[67] R. Claus,[67] M. R. Convery,[67] M. Cristinziani,[67] J. C. Dingfelder,[67] D. Dong,[67] J. Dorfan,[67] D. Dujmic,[67] W. Dunwoodie,[67] S. Fan,[67] R. C. Field,[67] T. Glanzman,[67] S. J. Gowdy,[67] T. Hadig,[67] V. Halyo,[67] C. Hast,[67] T. Hryn'ova,[67] W. R. Innes,[67] M. H. Kelsey,[67] P. Kim,[67] M. L. Kocian,[67] D. W. G. S. Leith,[67] J. Libby,[67] S. Luitz,[67] V. Luth,[67] H. L. Lynch,[67] H. Marsiske,[67] R. Messner,[67] D. R. Muller,[67] C. P. O'Grady,[67] V. E. Ozcan,[67] A. Perazzo,[67] M. Perl,[67] B. N. Ratcliff,[67] A. Roodman,[67] A. A. Salnikov,[67] R. H. Schindler,[67] J. Schwiening,[67] A. Snyder,[67] J. Stelzer,[67] D. Su,[67] M. K. Sullivan,[67] K. Suzuki,[67] S. Swain,[67] J. M. Thompson,[67] J. Va'vra,[67] M. Weaver,[67] W. J. Wisniewski,[67] M. Wittgen,[67] D. H. Wright,[67] A. K. Yarritu,[67] K. Yi,[67] C. C. Young,[67] P. R. Burchat,[68] A. J. Edwards,[68] S. A. Majewski,[68] B. A. Petersen,[68] C. Roat,[68] M. Ahmed,[69] S. Ahmed,[69] M. S. Alam,[69] J. A. Ernst,[69] M. A. Saeed,[69] F. R. Wappler,[69] S. B. Zain,[69] W. Bugg,[70] M. Krishnamurthy,[70] S. M. Spanier,[70] R. Eckmann,[71] J. L. Ritchie,[71] A. Satpathy,[71] R. F. Schwitters,[71] J. M. Izen,[72] I. Kitayama,[72] X. C. Lou,[72] S. Ye,[72] F. Bianchi,[73] M. Bona,[73] F. Gallo,[73] D. Gamba,[73] M. Bomben,[74] L. Bosisio,[74] C. Cartaro,[74] F. Cossutti,[74] G. Della Ricca,[74] S. Dittongo,[74] S. Grancagnolo,[74] L. Lanceri,[74] L. Vitale,[74] F. Martinez-Vidal,[75] R. S. Panvini,[76,‡] Sw. Banerjee,[77] B. Bhuyan,[77] C. M. Brown,[77] D. Fortin,[77] K. Hamano,[77] R. Kowalewski,[77] J. M. Roney,[77] R. J. Sobie,[77] J. J. Back,[78] P. F. Harrison,[78] T. E. Latham,[78] G. B. Mohanty,[78] H. R. Band,[79] X. Chen,[79] B. Cheng,[79] S. Dasu,[79] M. Datta,[79] A. M. Eichenbaum,[79] K. T. Flood,[79] M. Graham,[79] J. J. Hollar,[79] J. R. Johnson,[79] P. E. Kutter,[79] H. Li,[79] R. Liu,[79] B. Mellado,[79] A. Mihalyi,[79] Y. Pan,[79] R. Prepost,[79] P. Tan,[79] J. H. von Wimmersperg-Toeller,[79] S. L. Wu,[79] Z. Yu,[79] and H. Neal[80]

(*BABAR* Collaboration)

[1]*Laboratoire de Physique des Particules, F-74941 Annecy-le-Vieux, France*
[2]*IFAE, Universitat Autonoma de Barcelona, E-08193 Bellaterra, Barcelona, Spain*
[3]*Università di Bari, Dipartimento di Fisica and INFN, I-70126 Bari, Italy*
[4]*Institute of High Energy Physics, Beijing 100039, China*
[5]*Institute of Physics, University of Bergen, N-5007 Bergen, Norway*
[6]*Lawrence Berkeley National Laboratory, Berkeley, California 94720, USA and University of California, Berkeley, California 94720, USA*
[7]*University of Birmingham, Birmingham, B15 2TT, United Kingdom*
[8]*Institut für Experimentalphysik 1, Ruhr Universität Bochum, D-44780 Bochum, Germany*
[9]*University of Bristol, Bristol BS8 1TL, United Kingdom*
[10]*University of British Columbia, Vancouver, British Columbia V6T 1Z1, Canada*
[11]*Brunel University, Uxbridge, Middlesex UB8 3PH, United Kingdom*
[12]*Budker Institute of Nuclear Physics, Novosibirsk 630090, Russia*
[13]*University of California at Irvine, Irvine, California 92697, USA*
[14]*University of California at Los Angeles, Los Angeles, California 90024, USA*
[15]*University of California at Riverside, Riverside, California 92521, USA*
[16]*University of California at San Diego, La Jolla, California 92093, USA*
[17]*University of California at Santa Barbara, Santa Barbara, California 93106, USA*
[18]*Institute for Particle Physics, University of California at Santa Cruz, Santa Cruz, California 95064, USA*
[19]*California Institute of Technology, Pasadena, California 91125, USA*

[20]University of Cincinnati, Cincinnati, Ohio 45221, USA
[21]University of Colorado, Boulder, Colorado 80309, USA
[22]Colorado State University, Fort Collins, Colorado 80523, USA
[23]Institut für Physik, Universität Dortmund, D-44221 Dortmund, Germany
[24]nstitut für Kern- und Teilchenphysik, Technische Universität Dresden, ID-01062 Dresden, Germany
[25]Ecole Polytechnique, LLR, F-91128 Palaiseau, France
[26]University of Edinburgh, Edinburgh EH9 3JZ, United Kingdom
[27]Dipartimento di Fisica and INFN, Università di Ferrara, I-44100 Ferrara, Italy
[28]Laboratori Nazionali di Frascati dell'INFN, I-00044 Frascati, Italy
[29]Dipartimento di Fisica and INFN, Università di Genova, I-16146 Genova, Italy
[30]Harvard University, Cambridge, Massachusetts 02138, USA
[31]Physikalisches Institut, Universität Heidelberg, Philosophenweg 12, D-69120 Heidelberg, Germany
[32]Imperial College London, London, SW7 2AZ, United Kingdom
[33]University of Iowa, Iowa City, Iowa 52242, USA
[34]Iowa State University, Ames, Iowa 50011-3160, USA
[35]Laboratoire de l'Accélérateur Linéaire, F-91898 Orsay, France
[36]Lawrence Livermore National Laboratory, Livermore, California 94550, USA
[37]University of Liverpool, Liverpool L69 72E, United Kingdom
[38]Queen Mary, University of London, E1 4NS, United Kingdom
[39]Royal Holloway and Bedford New College, University of London, Egham, Surrey TW20 0EX, United Kingdom
[40]University of Louisville, Louisville, Kentucky 40292, USA
[41]University of Manchester, Manchester M13 9PL, United Kingdom
[42]University of Maryland, College Park, Maryland 20742, USA
[43]University of Massachusetts, Amherst, Massachusetts 01003, USA
[44]Massachusetts Institute of Technology, Laboratory for Nuclear Science, Cambridge, Massachusetts 02139, USA
[45]McGill University, Montréal, Quebec H3A 2T8, Canada
[46]Dipartimento di Fisica and INFN, Università di Milano, I-20133 Milano, Italy
[47]University of Mississippi, University, Mississippi 38677, USA
[48]Laboratoire René J. A. Lévesque, Université de Montréal, Montréal, Quebec, Canada H3C 3J7
[49]Mount Holyoke College, South Hadley, Massachusetts 01075, USA
[50]Dipartimento di Scienze Fisiche and INFN, Università di Napoli Federico II, I-80126, Napoli, Italy
[51]NIKHEF, National Institute for Nuclear Physics and High Energy Physics, NL-1009 DB Amsterdam, The Netherlands
[52]University of Notre Dame, Notre Dame, Indiana 46556, USA
[53]Ohio State University, Columbus, Ohio 43210, USA
[54]University of Oregon, Eugene, Oregon 97403, USA
[55]Dipartimento di Fisica and INFN, Università di Padova, I-35131 Padova, Italy
[56]Laboratoire de Physique Nucléaire et de Hautes Energies, Universités Paris VI et VII, F-75252 Paris, France
[57]University of Pennsylvania, Philadelphia, Pennsylvania 19104, USA
[58]Dipartimento di Fisica and INFN, Università di Perugia, I-06100 Perugia, Italy
[59]Dipartimento di Fisica, Scuola Normale Superiore and INFN, Università di Pisa, I-56127 Pisa, Italy
[60]Prairie View A&M University, Prairie View, Texas 77446, USA
[61]Princeton University, Princeton, New Jersey 08544, USA
[62]Dipartimento di Fisica and INFN, Università di Roma La Sapienza, I-00185 Roma, Italy
[63]Universität Rostock, D-18051 Rostock, Germany
[64]Rutherford Appleton Laboratory, Chilton, Didcot, Oxon, OX11 0QX, United Kingdom
[65]DSM/Dapnia, CEA/Saclay, F-91191 Gif-sur-Yvette, France
[66]University of South Carolina, Columbia, South Carolina 29208, USA
[67]Stanford Linear Accelerator Center, Stanford, California 94309, USA
[68]Stanford University, Stanford, California 94305-4060, USA
[69]State University of New York, Albany, New York 12222, USA
[70]University of Tennessee, Knoxville, Tennessee 37996, USA
[71]University of Texas at Austin, Austin, Texas 78712, USA
[72]University of Texas at Dallas, Richardson, Texas 75083, USA
[73]Dipartimento di Fisica Sperimentale and INFN, Università di Torino, I-10125 Torino, Italy
[74]Dipartimento di Fisica and INFN, Università di Trieste, I-34127 Trieste, Italy
[75]IFIC, Universitat de Valencia-CSIC, E-46071 Valencia, Spain
[76]Vanderbilt University, Nashville, Tennessee 37235, USA
[77]University of Victoria, Victoria, British Columbia V8W 3P6, Canada
[78]Department of Physics, University of Warwick, Coventry CV4 7AL, United Kingdom
[79]University of Wisconsin, Madison, Wisconsin 53706, USA
[80]Yale University, New Haven, Connecticut 06511, USA

(Received 23 June 2005; published 1 November 2005)

A search for lepton-flavor and lepton-number violation in the decay of the tau lepton into one charged lepton and two charged hadrons is performed using 221.4 fb^{-1} of data collected at an e^+e^- center-of-mass energy of 10.58 GeV with the *BABAR* detector at the SLAC PEP-II storage ring. In all 14 decay modes considered, the observed data are compatible with background expectations, and upper limits are set in the range $\mathcal{B}(\tau \to \ell hh') < (0.7 - 4.8) \times 10^{-7}$ at 90% confidence level.

DOI: 10.1103/PhysRevLett.95.191801 PACS numbers: 13.35.Dx, 11.30.Fs, 11.30.Hv, 14.60.Fg

Lepton-flavor violation (LFV) involving charged leptons has never been observed, and there are stringent experimental limits from muon decays: $\mathcal{B}(\mu \to e\gamma) < 1.2 \times 10^{-11}$ [1] and $\mathcal{B}(\mu \to eee) < 1.0 \times 10^{-12}$ [2] at 90% confidence level (C.L.). In tau decays, the most stringent limits on LFV are $\mathcal{B}(\tau \to \mu\gamma) < 6.8 \times 10^{-8}$ and $\mathcal{B}(\tau \to \ell\ell\ell) < (1 - 3) \times 10^{-7}$ at 90% C.L. [3,4]. While forbidden in the standard model (SM), many extensions to the SM predict enhanced LFV in tau decays with respect to muon decays with branching fractions from 10^{-10} up to the current experimental limits [5]. Observation of LFV in tau decays would be a clear signature of physics beyond the SM, while nonobservation will provide further constraints on theoretical models.

This Letter presents the results of a search for lepton-flavor violation in the neutrinoless decays $\tau^- \to \ell^- h^+ h'^-$ where ℓ represents an electron or muon and h represents a pion or kaon [6]. In addition, a search is also performed for the decays $\tau^- \to \ell^+ h^- h'^-$ which also violate lepton-number conservation. All possible lepton and hadron combinations consistent with charge conservation are considered, leading to 14 distinct decay modes as shown in Table I. The best existing limits on the branching fractions for these decay modes currently come from CLEO: (2–8) $\times 10^{-6}$ at 90% C.L. [7].

The data used in this analysis were collected with the *BABAR* detector at the SLAC PEP-II asymmetric-energy e^+e^- storage ring. The data sample consists of 221.4 fb^{-1} recorded at a luminosity-weighted center-of-mass energy $\sqrt{s} = 10.58$ GeV. With an estimated cross section for tau pairs of $\sigma_{\tau\tau} = (0.89 \pm 0.02)$ nb [8], this data sample contains nearly 4×10^8 tau decays.

Charged-particle (track) momenta are measured with a 5-layer double-sided silicon vertex tracker and a 40-layer drift chamber inside a 1.5 T superconducting solenoidal magnet. An electromagnetic calorimeter (EMC) consisting of 6580 CsI(Tl) crystals is used to identify electrons and photons, a ring-imaging Cherenkov detector (DIRC) and energy loss in the tracking system are used to identify charged hadrons, and the instrumented magnetic flux return (IFR) is used to identify muons. Further details on the *BABAR* detector are found in Ref. [9].

A Monte Carlo (MC) simulation of neutrinoless tau decays is used to study the performance of this analysis. Simulated $\tau^+\tau^-$ events including higher-order radiative corrections are generated using the KK2F MC generator [8], with one tau decaying to one lepton and two hadrons with a 3-body phase space distribution, while the second tau decay is simulated with TAUOLA [10] according to measured rates [11]. Final state radiative effects are simulated for all decays using PHOTOS [12]. The detector response is simulated with GEANT [13], and the simulated events are reconstructed in the same manner as data.

Candidate signal events are required to have a 1–3 topology, where one tau decay yields one charged particle (1 prong), while the other tau decay yields three charged particles (3 prong). Four well reconstructed tracks are required with zero net charge, originating from a common region consistent with $\tau\tau$ production and decay. Pairs of oppositely charged tracks, likely to be from photon conversions in the detector material, are ignored if their e^+e^- invariant mass is less than 30 MeV/c^2. The event is divided into hemispheres using the plane perpendicular to the thrust axis, calculated from the observed track momenta and EMC energy deposits, in the center-of-mass (c.m.) frame. One hemisphere must contain exactly one track while the other must contain exactly three.

TABLE I. Efficiency estimates, the number of expected background events ($N_{\rm bgd}$) in the signal region (with total uncertainties), the number of observed events ($N_{\rm obs}$) in the signal region, and the 90% C.L. upper limit on the branching fraction for each decay mode.

Mode	Efficiency [%]	$N_{\rm bgd}$	$N_{\rm obs}$	UL at 90% C.L.
$e^-K^+K^-$	3.77 ± 0.16	0.22 ± 0.06	0	1.4×10^{-7}
$e^-K^+\pi^-$	3.08 ± 0.13	0.32 ± 0.08	0	1.7×10^{-7}
$e^-\pi^+K^-$	3.10 ± 0.13	0.14 ± 0.06	1	3.2×10^{-7}
$e^-\pi^+\pi^-$	3.30 ± 0.15	0.81 ± 0.13	0	1.2×10^{-7}
$\mu^-K^+K^-$	2.16 ± 0.12	0.24 ± 0.07	0	2.5×10^{-7}
$\mu^-K^+\pi^-$	2.97 ± 0.16	1.67 ± 0.29	2	3.2×10^{-7}
$\mu^-\pi^+K^-$	2.87 ± 0.16	1.04 ± 0.18	1	2.6×10^{-7}
$\mu^-\pi^+\pi^-$	3.40 ± 0.19	2.99 ± 0.41	3	2.9×10^{-7}
$e^+K^-K^-$	3.85 ± 0.16	0.04 ± 0.04	0	1.5×10^{-7}
$e^+K^-\pi^-$	3.19 ± 0.14	0.16 ± 0.06	0	1.8×10^{-7}
$e^+\pi^-\pi^-$	3.40 ± 0.15	0.41 ± 0.10	1	2.7×10^{-7}
$\mu^+K^-K^-$	2.06 ± 0.11	0.07 ± 0.10	1	4.8×10^{-7}
$\mu^+K^-\pi^-$	2.85 ± 0.16	1.54 ± 0.25	1	2.2×10^{-7}
$\mu^+\pi^-\pi^-$	3.30 ± 0.18	1.46 ± 0.27	0	0.7×10^{-7}

One of the charged particles found in the 3-prong hemisphere must be identified as either an electron or muon candidate. Electrons are identified using the ratio of observed EMC energy to track momentum (E/p), the shape of the shower in the EMC, and the ionization loss in the tracking system (dE/dx). Muons are identified by hits in the IFR and small energy deposits in the EMC. Each of the other two charged particles found in the 3-prong hemisphere must be identified as either a pion or a kaon, using information from the DIRC and dE/dx.

After event topology and particle identification requirements, there are significant backgrounds from light quark $q\bar{q}$ production and SM $\tau\tau$ events (without LFV), as well as small contributions from Bhabha, $\mu^+\mu^-$, and two-photon production of four charged particles. Additional selection criteria, largely the same for all 14 signal channels, are applied as follows. No photon candidates, identified as EMC energy deposits unassociated to a track, with $E_\gamma > 100$ MeV are allowed. This restriction removes $q\bar{q}$ backgrounds and SM $\tau\tau$ events. The total transverse momentum of the event in the c.m. frame must be greater than 0.2 GeV/c, while the polar angle of the missing momentum in the laboratory frame is required to be in the range $[0.25, 2.4]$ radians. These two requirements are effective at reducing two-photon and Bhabha backgrounds. The mass of the 1-prong hemisphere calculated from the four-momentum of the track in the 1-prong hemisphere and the missing momentum in the event, is required to be in the range $[0.6, 1.9]$ GeV/c^2 for ehh' candidates and $[0.8, 1.9]$ GeV/c^2 for $\mu hh'$ candidates. The 1-prong mass requirement is particularly effective at removing $q\bar{q}$ backgrounds as well as the remaining two-photon contribution. To reduce Bhabha backgrounds, the momentum of the 1-prong track in the c.m. frame is required to be less than 4.5 GeV/c for the $e\pi\pi$ candidates. In addition, particle identification vetoes are applied to specific selection channels. For all decay modes, lepton and pion candidates must not pass the kaon identification as well. For the ehh' decay modes, except for eKK, the 1-prong track must not be identified as an electron. This requirement is useful to reduce possible contamination from Bhabhas.

To further reduce backgrounds, candidate signal events are required to have an invariant mass and total energy in the 3-prong hemisphere consistent with the neutrinoless decay of a tau lepton. These quantities are calculated from the observed track momenta assuming the corresponding lepton and hadron masses for each decay mode. The mass difference and energy difference are defined as $\Delta M \equiv M_{\rm rec} - m_\tau$ and $\Delta E \equiv E_{\rm rec}^{\rm c.m.} - E_{\rm beam}^{\rm c.m.}$, where $M_{\rm rec}$ is the reconstructed 3-prong invariant mass, $m_\tau = 1.777$ GeV/c^2 is the tau mass [14], $E_{\rm rec}^{\rm c.m.}$ is the reconstructed 3-prong total energy in the c.m. frame, and $E_{\rm beam}^{\rm c.m.}$ is the c.m. beam energy. Rectangular signal regions are defined separately for each decay mode in the $(\Delta M, \Delta E)$ plane. For the $\mu hh'$ modes, ΔM is required to be in the range $[-20, +20]$ MeV/c^2, while for the ehh' modes the range is $[-30, +20]$ MeV/c^2 to account for radiative losses. For all 14 decay modes, ΔE must be in the range $[-100, +50]$ MeV.

These signal region boundaries are optimized to provide the smallest expected upper limits on the branching fractions in the background-only hypothesis. These expected upper limits are estimated using only MC simulations, not candidate events in data. To avoid bias, a blind analysis procedure was adopted with the number of data events in the signal region remaining unknown until the selection criteria were finalized and all systematic studies had been performed. Figure 1 shows the observed data for all 14 selection channels, along with the signal region boundaries and the expected signal distributions.

The dominant remaining backgrounds are low multiplicity $q\bar{q}$ events and SM $\tau\tau$ events. These background classes have unique distributions in the $(\Delta M, \Delta E)$ plane: $q\bar{q}$ events populate the plane uniformly, while $\tau\tau$ backgrounds are restricted to negative values of both ΔM and ΔE. Backgrounds from Bhabha, $\mu\mu$, and two-photon

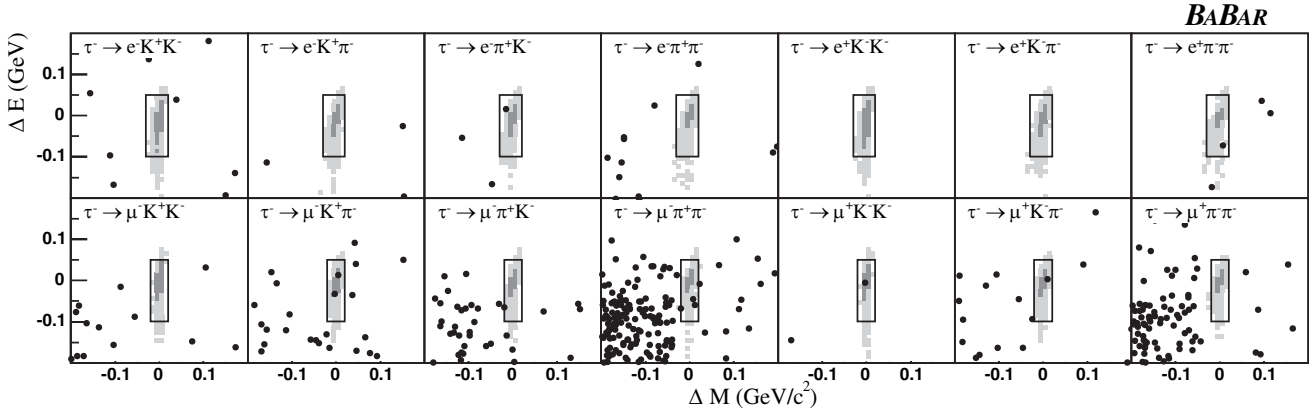

FIG. 1. Observed data shown as dots in the $(\Delta M, \Delta E)$ plane and the boundaries of the signal region for each decay mode. The dark and light shading indicates contours containing 50% and 90% of the selected MC signal events, respectively.

events are found to be negligible. For each background class, a probability density function (PDF) describing the shape of the background distribution in the $(\Delta M, \Delta E)$ plane is determined by fitting an analytic function to the Monte Carlo prediction as described in more detail below. These PDFs are then combined with normalization coefficients determined from an unbinned maximum likelihood fit to the observed data in the $(\Delta M, \Delta E)$ plane in a sideband (SB) region. The resulting function describes the event rate observed in the SB region and is used to predict the expected background rate in the signal region. The SB region is defined as the rectangle, excluding the signal region, bounding ΔM in the range $[-0.7, +0.4]$ GeV$/c^2$ for ehh' final states and $[-0.4, +0.4]$ GeV$/c^2$ for $\mu hh'$ final states, while ΔE must be in the range $[-0.7, +0.4]$ GeV. The PDF shape determinations and SB fits are performed separately for each of the 14 decay modes.

For the $q\bar{q}$ backgrounds, a PDF is constructed from the product of two functions $P_{M'}$ and $P_{E'}$, where the coordinates $(\Delta M', \Delta E')$ have been rotated slightly from $(\Delta M, \Delta E)$ to better fit the expected distributions. The function $P_{M'}(\Delta M')$ is a Gaussian and the function $P_{E'}(\Delta E') = (1 - x/\sqrt{1 + x^2})(1 + a_1 x + a_2 x^2 + a_3 x^3)$ where $x = (\Delta E' - a_4)/a_5$ and a_i are fit parameters. The resulting $q\bar{q}$ PDF is described by eight fit parameters, including the rotation angle, which are determined by fits to MC $q\bar{q}$ background samples for each decay mode. For the $\tau\tau$ PDF, the function $P_{M'}(\Delta M')$ is the sum of two Gaussians with different widths above and below the peak, while the functional form of $P_{E'}(\Delta E')$ is the same as the $q\bar{q}$ PDF above. To properly model the wedge-shaped kinematic limit in tau decays, a coordinate transformation of the form $\Delta M' = \cos\beta_1 \Delta M + \sin\beta_1 \Delta E$ and $\Delta E' = \cos\beta_2 \Delta E - \sin\beta_2 \Delta M$ is performed. In total there are 12 free parameters describing this PDF, and all are determined by fits to MC $\tau\tau$ samples.

With the shapes of the two background PDFs determined, an unbinned maximum likelihood fit to the data in the SB region is used to find the expected rate of each background type in the signal region. Extensive MC studies show that these PDF functions adequately describe the predicted background shapes near the signal regions. The accuracy of these predictions is verified by comparing to data in regions neighboring the signal region in the $(\Delta M, \Delta E)$ plane where no signal is expected. Expected backgrounds are shown in Table I, and an example of the background prediction compared to the observed data is shown in Fig. 2.

The efficiency of the selection for signal events is estimated with a MC simulation of neutrinoless tau decays. About 40% of the MC signal events pass the initial 1–3 topology requirement, and 20% to 70% of these preselected events pass the particle identification (PID) criteria, depending upon the signal mode. The final efficiency for signal events to be found in the signal region after all

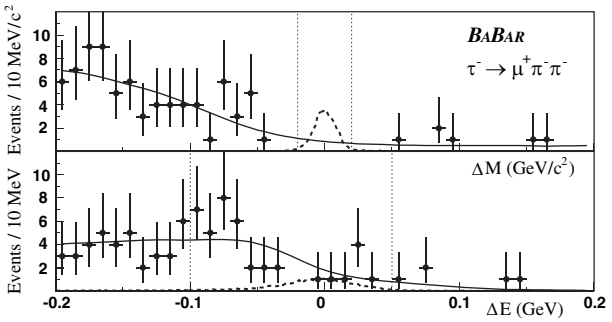

FIG. 2. Data (points) and background expectation (solid line) are shown for the $\mu^+\pi^-\pi^-$ candidates displayed in Fig. 1. Expected signal distributions for a branching fraction of 5×10^{-7} are also shown as the dashed curve. The vertical lines indicate the signal region.

requirements is shown in Table I for each decay mode and ranges from 2.1% to 3.8%. This efficiency includes the 85% branching fraction for 1-prong tau decays [11].

The PID selection efficiencies and misidentification rates are measured directly using tracks in kinematically-selected data control samples. These values are parametrized as a function of particle momentum, charge, polar angle, and azimuthal angle in the laboratory frame. The lepton-identification criteria have been designed to give very low misidentification rates at the expense of some efficiency loss. The electron ID is expected to be 81% efficient in signal ehh' events, with a mis-ID rate of 0.1% for pions and 0.2% for kaons in generic $\tau\tau$ events. The muon ID is 44% efficient for $\mu hh'$ signal events, with a mis-ID rate of 1.0% for pions and 0.4% for kaons. The hadronic identification is designed to classify the hadronic candidates as pions or kaons, but is not intended to distinguish hadrons from leptons. The pion ID is 92% efficient with a mis-ID rate of 12% for kaons, while the kaon ID is 81% efficient with a 1.4% mis-ID rate for pions.

The largest systematic uncertainty for the signal efficiency is the uncertainty in measuring particle ID efficiencies. This uncertainty (all uncertainties quoted are relative) is dominated by the statistical precision of the PID control samples, and ranges from 0.7% for $e^-\pi^+\pi^-$ to 3.8% for $\mu^- K^+ K^-$. The modeling of the tracking efficiency contributes an uncertainty of 2.5%, while the restriction on extra photons leads to an additional uncertainty of 2.4%. All other sources of uncertainty are found to be small, including the modeling of radiative effects, track momentum resolution, trigger performance, observables used in the selection criteria, and knowledge of the tau 1-prong branching fractions. No uncertainty is assigned for possible model dependence of the signal decay. The selection efficiency is found to be uniform within 20% across the Dalitz plane, provided the invariant mass for any pair of particles is less than 1.4 GeV$/c^2$.

Since the background levels are extracted directly from the data, systematic uncertainties on the background esti-

mation are directly related to the background normalization, parametrization, and the fit technique used. The finite data available in the SB region used to determine the background rates dominates the background uncertainty. Additional uncertainties of 10% are estimated by varying the fit procedure and changing the functional form of the background PDFs. The uncertainty on the branching fraction of SM tau decays with one or two kaons is also evaluated, and contributes less than 15% for all final states.

The numbers of events observed ($N_{\rm obs}$) and the background expectations ($N_{\rm bgd}$) are shown in Table I, with no significant excess observed. Upper limits on the branching fractions are calculated according to $\mathcal{B}_{\rm UL}^{90} = N_{\rm UL}^{90}/(2\varepsilon\mathcal{L}\sigma_{\tau\tau})$, where $N_{\rm UL}^{90}$ is the 90% C.L. upper limit for the number of signal events when $N_{\rm obs}$ events are observed with $N_{\rm bgd}$ background events expected. The quantities ε, $\mathcal{L}$, and $\sigma_{\tau\tau}$ are the selection efficiency, luminosity, and $\tau^+\tau^-$ cross section, respectively. The branching fraction upper limits are calculated including all uncertainties using the technique of Cousins and Highland [15] following the implementation of Barlow [16]. The estimates of $\mathcal{L}$ and $\sigma_{\tau\tau}$ are correlated [17], and the uncertainty on the product $\mathcal{L}\sigma_{\tau\tau}$ is 2.3%. The 90% C.L. upper limits on the $\tau \to \ell hh'$ branching fractions, shown in Table I, are in the range $(0.7\text{–}4.8) \times 10^{-7}$. These limits represent an order of magnitude improvement over the previous experimental bounds [7].

We are grateful for the excellent luminosity and machine conditions provided by our SLAC PEP-II colleagues, and for the substantial dedicated effort from the computing organizations that support *BABAR*. The collaborating institutions wish to thank SLAC for its support and kind hospitality. This work is supported by DOE and NSF (USA), NSERC (Canada), IHEP (China), CEA and CNRS-IN2P3 (France), BMBF and DFG (Germany), INFN (Italy), FOM (The Netherlands), NFR (Norway), MIST (Russia), and PPARC (United Kingdom). Individuals have received support from CONACyT (Mexico), A. P. Sloan Foundation, Research Corporation, and Alexander von Humboldt Foundation.

*Also with Università di Perugia, Dipartimento di Fisica, Perugia, Italy.
†Also with Università della Basilicata, Potenza, Italy.
‡Deceased.

[1] M. L. Brooks *et al.* (MEGA/LAMPF Collaboration), Phys. Rev. Lett. **83**, 1521 (1999).
[2] U. Bellgardt *et al.* (SINDRUM Collaboration), Nucl. Phys. **B299**, 1 (1988).
[3] B. Aubert *et al.* (*BABAR* Collaboration), Phys. Rev. Lett. **95**, 041802 (2005).
[4] B. Aubert *et al.* (*BABAR* Collaboration), Phys. Rev. Lett. **92**, 121801 (2004).
[5] E. Ma, Nucl. Phys. B, Proc. Suppl. **123**, 125 (2003).
[6] Throughout this Letter, charge conjugate decay modes are also implied.
[7] D. W. Bliss *et al.* (CLEO Collaboration), Phys. Rev. D **57**, 5903 (1998).
[8] B. F. Ward, S. Jadach, and Z. Was, Nucl. Phys. B, Proc. Suppl. **116**, 73 (2003).
[9] B. Aubert *et al.* (*BABAR* Collaboration), Nucl. Instrum. Methods Phys. Res., Sect. A **479**, 1 (2002).
[10] S. Jadach, Z. Was, R. Decker, and J. H. Kuhn, Comput. Phys. Commun. **76**, 361 (1993).
[11] S. Eidelman *et al.* (Particle Data Group), Phys. Lett. B **592**, 1 (2004).
[12] E. Barberio and Z. Was, Comput. Phys. Commun. **79**, 291 (1994).
[13] S. Agostinelli *et al.* (GEANT4 Collaboration), Nucl. Instrum. Methods Phys. Res., Sect. A **506**, 250 (2003).
[14] J. Z. Bai *et al.* (BES Collaboration), Phys. Rev. D **53**, 20 (1996).
[15] R. D. Cousins and V. L. Highland, Nucl. Instrum. Methods Phys. Res., Sect. A **320**, 331 (1992).
[16] R. Barlow, Comput. Phys. Commun. **149**, 97 (2002).
[17] The luminosity is measured using the observed $\mu^+\mu^-$ rate, and the $\mu^+\mu^-$ and $\tau^+\tau^-$ cross sections are both estimated with KK2F.